

# A Search for Biomolecules in Sagittarius B2 (LMH) with the ATCA

P. A. Jones<sup>1</sup>, \* M. R. Cunningham<sup>1</sup>, P. D. Godfrey<sup>2</sup> and D. M. Cragg<sup>2</sup>

<sup>1</sup>School of Physics, University of New South Wales, NSW 2052, Australia

<sup>2</sup>School of Chemistry, PO Box 23, Monash University, Clayton, Victoria 3800, Australia

arXiv:astro-ph/0610273v1 10 Oct 2006

Accepted . Received ; in original form

## ABSTRACT

We have used the Australia Telescope Compact Array to conduct a search for the simplest amino acid, glycine (conformers I and II), and the simple chiral molecule propylene oxide at 3-mm in the Sgr B2 LMH. We searched 15 portions of spectrum between 85 and 91 GHz, each of 64 MHz bandwidth, and detected 58 emission features and 21 absorption features, giving a line density of 75 emission lines and 25 absorption lines per GHz stronger than the  $5\sigma$  level of 110 mJy. Of these, 19 are transitions previously detected in the interstellar medium, and we have made tentative assignments of a further 23 features to molecular transitions. However, as many of these involve molecules not previously detected in the ISM, these assignments cannot be regarded with confidence. Given the median line width of 6.5 km/s in Sgr B2 LMH, we find that the spectra have reached a level where there is line confusion, with about 1/5 of the band being covered with lines. Although we did not confidently detect either glycine or propylene oxide, we can set  $3\sigma$  upper limits for most transitions searched. We also show that if glycine is present in the Sgr B2 LMH at the level of  $N = 4 \times 10^{14}$  cm<sup>-2</sup> found by Kuan et al. (2003) in their reported detection of glycine, it should have been easily detected with the ATCA synthesized beam size of 17.0 x 3.4 arcsec<sup>2</sup>, if it were confined to the scale of the LMH continuum source (< 5 arcsec). This thus puts a strong upper limit on any small-scale glycine emission in Sgr B2, for both of conformers I and II.

**Key words:** ISM:molecules - radio lines:ISM - ISM:individual:Sgr B2

## 1 INTRODUCTION

It is generally presumed that life on Earth developed from an initial reservoir of simpler prebiotic organic material such as amino acids, fatty acids and sugars. What is not clear is whether the chemical evolution to produce this initial reservoir occurred on the early Earth, in the pre-solar nebula, or even earlier in interstellar molecular clouds. In fact, a significant body of work exists which suggests that the necessary chemical evolution could not have taken place on the early Earth itself (Joyce et al. 1984; Bailey et al 1998), suggesting that the chemical evolution took place within the pre-solar nebula, with the organic material being delivered to the Earth by meteorites and comets during the phase of bombardment.

Although there is expected to be some chemical and physical processing of material originating in the ISM,

through the pre-solar nebula, into cometary and meteoritic material, and on to the surface of a planet, a study of the most complex molecules in the ISM is an important step in determining how likely it is that the reservoir of molecules from which life evolved originated in the pre-solar nebula. Indeed, a large number of surprisingly complex molecules, including amino acids, have been found in carbonaceous chondrite meteorites (see e.g. Wirick et al. 2006), which are thought to be relatively unprocessed remnants of the presolar nebula.

In this paper we describe an Australia Telescope Compact Array (ATCA) search for two biologically important molecules: the simplest amino acid glycine ( $\text{NH}_2\text{CH}_2\text{COOH}$ ), and the cyclic molecule propylene oxide ( $\text{c}-\text{CH}_3\text{C}_2\text{H}_3\text{O}$ ) which is chiral. Chiral molecules are those where asymmetry in carbon atom placement within a molecule leads to two distinct forms (mirror images or enantiomers). Figure 1 shows the chemical structure of propylene oxide.

\* E-mail: Paul.Jones@csiro.au  
Maria.Cunningham@unsw.edu.au (MRC)

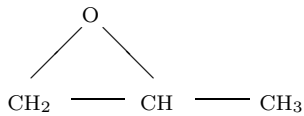


**Figure 1.** The chemical structure of the simple chiral molecule propylene oxide ( $c - \text{CH}_3\text{C}_2\text{H}_3\text{O}$ )

### 1.1 Other Searches for Glycine

There have been many searches for glycine in molecular clouds, dating back over 20 years (eg. Brown et al. 1979, Hollis et al. 1980, Snyder et al. 1983) with negative or ambiguous results. Miao et al. (1994) and Snyder (1997) reported a possible detection of a 90 GHz transition of glycine in Sgr B2 (N) with BIMA and OVRO (interferometers). There were some caveats in Snyder (1997) due to uncertainty in the glycine line rest frequency, the different velocity components in Sgr B2 (N), and the confusion with other lines. Combes, Rieu & Wlodarczak (1996) used the IRAM 30-m telescope (single dish) for the positions Orion SiO and Sgr B2 (OH) and concluded that the confusion of lines in the millimetre spectra, particularly in the Orion position, could make the detection of glycine impossible, as the glycine lines would be below the confusion limit.

Kuan et al. (2003, 2004a, 2004b) have reported the detection of glycine in Sgr B2 (N-LMH), Orion KL and W51 e1/e2 using the NRAO 12-m telescope. They used the detailed comparison of lines in the different sources to help solve the problem of “interloper” lines of other species. The use of rotation diagrams to provide a quantitative comparison of many detections and upper limits of the glycine lines for all three sources gives greater confidence in the results. The total column density of glycine conformer I determined by Kuan et al. (2003) in Sgr B2 (N-LMH) is  $N = 4 \times 10^{14} \text{ cm}^{-2}$  and rotational temperature  $T = 75 \text{ K}$ .

This reported detection of Kuan et al. (2003) has been disputed in a paper by Snyder et al. (2005), who use unpublished NRAO 12-m data, and published SEST data from Nummelin et al. (1998) to show that upper limits from non-detections of glycine lines quite stringently rule out glycine in the three sources at the level reported by Kuan et al. (2003) unless present as the higher energy conformer II. In addition, they argue how random coincidences of lines misidentified as glycine could lead to a plausible looking, but spurious, fit to lines in a rotation diagram.

### 1.2 The Importance of Chiral Molecules

Investigations of primitive mechanisms of self-replication that involve RNA only, indicate the need for a reservoir of homochiral (having like chirality) organic molecules on the early Earth, before living organisms could evolve (Joyce et al. 1984). An excess of about 10 % in one enantiomer over the other (L over D in the case of amino acids on the Earth) is needed for RNA template reproduction to work.

Non-biological processes always create chiral organic

molecules in a racemic mix (equal numbers of both handednesses) and there are no known abiotic mechanisms operating on the surface of the Earth to generate the required enantiomeric excess. Therefore, an extraterrestrial origin for the prebiotic molecules needed to seed life on Earth is likely if we accept the hypothesis that primitive reproduction involved only RNA.

An extraterrestrial mechanism for producing the requisite homochirality is necessary. The most likely mechanism is circularly polarized UV radiation in the ISM, which is known to be capable of generating an enantiomeric excess by selectively destroying one enantiomer over the other (Bai-ley et al 1998).

Regrettably radio astronomy cannot distinguish the mirror image molecular forms, which in different concentrations would signal chiral imbalance, but it can potentially detect the presence of molecules capable of this property. To date, no molecules possessing a chiral centre have been detected in the ISM. Glycine is not a chiral molecule, and our search for biologically important chiral molecules with the ATCA and Mopra is focusing on propylene oxide. The simpler, non-chiral, but chemically related cyclic species ethylene oxide ( $c - \text{C}_2\text{H}_4\text{O}$ ) has already been detected in Sgr B2N (Dickens et al. 1997).

### 1.3 Our Search Strategy

Two developments prompted this search for glycine and propylene oxide:

- Firstly, we have been able to use laboratory measured values of the rest frequencies of glycine and propylene oxide transitions between 85 and 115 GHz rather than the less accurate calculated values (Lovas et al. 1995) on which previous searched at 3 mm have had to rely. The measurements were made at the School of Chemistry, Monash University, using a purpose-built Stark-modulated free-jet microwave absorption spectrometer of a design similar to that described previously (Brown et al. 1988). These measured values have an uncertainty of around only 0.07 km/s in the central velocity of a transition <sup>1</sup>.

- Secondly, the new capabilities of the ATCA at millimetre wavelengths allows a search at high spatial resolution, minimising beam dilution effects and, as an interferometer, filtering out confusing lines from the extended gas within the beam.

Our search has a multi-pronged approach, involving both single dish and interferometer observations of multiple frequencies within the 3-mm band. The position Sgr B2 (LMH) is of small diameter (<5 arcseconds) and has so far provided detections of the related complex molecules methyl formate and acetic acid (which is a precursor to glycine in some reaction networks). These molecules seem to be confined to the LMH. However, another similar molecule, glycolaldehyde (Hollis et al. 2001), was found to be extended in the Sgr B2 (N) molecular cloud, with very low concentrations in the LMH. These three molecules are believed to have a common origin with glycine (Sorrell 2001) based on a

<sup>1</sup> The new laboratory measurements are not yet publically available. Enquiries can be addressed to the authors

model of chemical reactions in icy grain mantles. It is therefore important to search for glycine in both extended and compact dense molecular gas.

We are thus using both the ATCA and the single dish Mopra radio telescope. The Mopra telescope, jointly operated by the ATNF CSIRO, and the University of New South Wales, Australia, has a 22-m diameter, making it the largest single dish telescope operating at 3-mm in the southern hemisphere. Mopra results will be discussed in a subsequent paper.

In the laboratory, glycine can adopt more than one conformation or spatial arrangement of the groups. Since it is uncertain which conformer of glycine may be present in the ISM, we searched for lines from both conformer I and conformer II (Lovas et al. 1995). Conformer I has lower energy than II by around  $E/hc = 700$  cm $^{-1}$  (Lovas et al. 1995), but conformer II has a larger dipole moment and hence stronger lines. There is a significant energy barrier between conformers I and II, since to go from one to the other requires breaking a hydrogen bond rather than just an internal rotation. The energy barrier is estimated theoretically at around  $E/hc = 5000$  cm $^{-1}$  or  $E/k = 7000K$  (Godfrey, Brown & Rodgers 1996). At interstellar temperatures the rate of tunnelling through the barrier will be low. If glycine is formed at low temperatures on grain surfaces, it may be stuck in the original conformation, and if the formation chemical processes favoured conformer II, it would relax only very slowly into the lower energy conformer I. Thus it is worthwhile searching for both conformers.

## 2 ATCA OBSERVATIONS AND DATA REDUCTION

Observations were made with the Australia Telescope Compact Array, in 2002 and 2003, during the southern Winter period of conditions appropriate for 3-mm observations. The log of observations is given in table 1.

During this 2002 and 2003 period, the 3-mm system installed on the ATCA was an interim system using only three of the six ATCA antennas, rather than the five antennas (on the 3-km EW track and NS spur) of the final system. Also, the interim local oscillator (LO) system for the 3-mm band did not allow the full tuning range 85 - 105 GHz of the final system. In the interim system the LO was fixed at 80.505 GHz, and the intermediate frequency (IF) passed through the existing C-band (4.4 - 6.8 GHz) or X-band (8.0 - 10.8 GHz) filters, giving the sky frequency coverage 84.906 - 87.305 and 88.506 - 91.305 GHz.

We selected the strongest predicted lines of glycine, conformers I and II, and propylene oxide in the available ATCA 3-mm frequency range, based on LTE calculations at 10 K and 50 K. The correlator configuration was two simultaneous bands of 64 MHz, each of 128 channels of bandwidth 0.5 MHz. Some of the bands included two or more biomolecule lines, so we covered 27 lines in 15 bands as shown in table 1.

Sagittarius B2, at declination  $-28^\circ$  passes nearly overhead at the ATCA, but we did not observe below an elevation of around  $30^\circ$ , since the phase errors and attenuation are worse at low elevation. The hour-angle coverage was therefore around 8 hours per observation, but the integration

**Table 1.** Log of ATCA observations, frequency bands and lines searched. The frequencies quoted are from new laboratory measurements made at the School of Chemistry, Monash University. The corresponding transitions are listed in table 4. The asterisk in column 4 denotes the line used as rest frequency for the velocity scale when more than one line was in the observed band. ID specifies the molecule, propylene oxide (PO) or glycine (G), and conformer, I or II (glycine only), with this transition frequency. Strength is a measure of the intensity predicted at 10 K and 50 K (10 K if only one number is given), relative to a value of 100 for the strongest line of that species in the 80-115 GHz range.

| Band Label | Dates                      | Arrays used  | Line Freq. (GHz)                              | ID                       | Strength 10/50 K                 |
|------------|----------------------------|--------------|---|--------------------------|----------------------------------|
| 85477      | 2003 Jun 06<br>2003 Jul 03 | H75<br>EW214 | 85.48422                                      | PO                       | 27                               |
| 86267      | 2003 Jun 06<br>2003 Jul 03 | H75<br>EW214 | 86.262231*<br>86.283667                       | G II<br>G II             | 27/51<br>27/51                   |
| 86374      | 2003 Jun 06<br>2003 Jul 03 | H75<br>EW214 | 86.379992                                     | G II                     | 74/82                            |
| 86709      | 2002 Jun 06<br>2002 Aug 18 | EW352<br>H75 | 86.72160*<br>86.716051                        | PO<br>G II               | 29<br>74/82                      |
| 86754      | 2002 Jun 06                | EW352        |   |                          |                                  |
| 86880      | 2003 Jun 06<br>2003 Jul 03 | H75<br>EW214 | 86.88593                                      | G I                      | 80/61                            |
| 86954      | 2002 Jun 06<br>2002 Aug 18 | EW352<br>H75 | 86.960812<br>86.967057*<br>86.978582          | G II<br>G II<br>G II     | 74/89<br>74/89<br>43/61          |
| 88587      | 2003 Jun 07<br>2003 Jul 02 | H75<br>EW214 | 88.59909<br>88.60199*                         | PO<br>PO                 | 8<br>8                           |
| 88761      | 2002 Aug 19                | H75          | 88.77871*<br>88.792618                        | PO<br>G II               | 15<br>4                          |
| 89502      | 2003 Jun 07<br>2003 Jul 02 | H75<br>EW214 | 89.50043<br>89.51220*<br>89.53550             | G I<br>G I<br>G I        | 62/67<br>22/44<br>23/44          |
| 89737      | 2003 Jun 07<br>2003 Jul 02 | H75<br>EW214 | 89.75055                                      | G I                      | 49/56                            |
| 89829      | 2002 Aug 19                | H75          | 89.87218<br>89.83184*<br>89.87571             | PO<br>G I<br>G I         | 23<br>63/67<br>34/52             |
| 90022      | 2002 Aug 19                | H75          | 90.03589<br>90.04311*<br>90.04967<br>90.05689 | G I<br>G I<br>G I<br>G I | 25/30<br>63/72<br>63/72<br>25/30 |
| 90451      | 2002 Aug 19                | H75          | 90.47516                                      | PO                       | 28                               |
| 90771      | 2003 Jun 07<br>2003 Jul 02 | H75<br>EW214 | 90.78355                                      | G I                      | 73/67                            |

**Table 2.** Resolution and sensitivity of the ATCA observations

| Band<br>Label | Beamsize<br>(arcsec <sup>2</sup> ) | PA<br>(deg) | RMS<br>(mJy/beam) |
|---------------|------------------------------------|-------------|-------------------|
| 85477         | 7.0×4.7                            | 0           | 18                |
| 86267         | 7.0×4.7                            | 0           | 16                |
| 86374         | 7.0×4.7                            | 0           | 16                |
| 86709         | 6.0×3.5                            | 0           | 14                |
| 86754         | 13.5×2.7                           | -22         | 20                |
| 86880         | 7.0×4.7                            | 0           | 21                |
| 86954         | 6.0×3.5                            | 0           | 15                |
| 88587         | 6.5×5.0                            | 0           | 35                |
| 88761         | 17.0×3.4                           | -84         | 33                |
| 89502         | 6.5×5.0                            | 0           | 26                |
| 89737         | 6.5×5.0                            | 0           | 26                |
| 89829         | 17.0×3.4                           | -81         | 26                |
| 90022         | 17.0×3.4                           | -83         | 22                |
| 90451         | 17.0×3.4                           | -85         | 31                |
| 90771         | 6.5×5.0                            | 0           | 27                |

time was more like half this when the observing overheads of pointing, phase calibrator, primary calibrator, bandpass calibrator and system temperature scans is taken into account. We used B1730-130 as the phase calibrator, with a cycle time of typically 10 minutes on source Sgr B2 and 2 minutes on B1730-130. Uranus was used as the primary calibrator. Either 3C279 or 1921-293 were used as bandpass calibrators. We typically combined 2 days of observations for each band, one with east-west spacings (EW214 or EW352) and one with north-south spacings (H75), to get better  $u,v$ -coverage. The range of antenna spacings was 30 to 120 m.

To increase the number of bands searched, albeit at the cost of reduced sensitivity, we generally timeshared between two frequency settings, getting four frequencies per observation (two settings times two simultaneous bands).

The data were reduced with the MIRIAD package, ATNF version (<http://www.atnf.csiro.au/computing/software/miriad/>). The gain-elevation dependence was corrected with task *elevcor*, and the primary flux scale set using the data for Uranus and the task *plboot*. There were some problems with the antenna baseline solutions for ATCA 3-mm observations, particularly during 2002, so we used phase self-calibration using the strong continuum flux of Sgr B2 (LMH).

The continuum emission was subtracted from the  $u,v$ -data with the Miriad task *imlin* by selecting the line-free channels. Continuum-free data cubes were made for each of the 15 bands, and the data cubes cleaned. The size of the clean restored beams are given in table 2. For the bands that had both EW and NS ATCA arrays, the beams are roughly circular, elongated by a factor around 1.5 north-south, but for the five bands with only one ATCA array, the beams are highly elongated north-south or east-west due to the rather poor  $u,v$ -coverage.

The data cubes were generated with velocity coordinates, with the biomolecule line rest frequencies given in table 1. Where two biomolecule lines are in the same band, the rest frequency used to convert from frequency to velocity is marked with an asterisk.

Continuum images were also made, using the line-free channels, by combining data for all the bands observed in 2002 and in 2003.

## 3 RESULTS

### 3.1 Sgr B2 3-mm continuum

The 3-mm continuum emission from Sgr B2 is resolved into two components by the ATCA, labelled N and N' by Kuan, Mehringer & Snyder (1996) from 3-mm BIMA observations of similar resolution. With only three baselines in the ATCA data, and uncertain calibration, the continuum image is in fair agreement with previous continuum observations. For the combined continuum data for 2003, the total flux from Gaussian fits to the two components is 7.1 Jy, compared to a total of 6.9 Jy at 87.9 GHz in Kuan et al. (1996). However, the fluxes of the two components in the 2003 ATCA image is 4.7 Jy for N and 2.4 Jy for N' compared to 3.7 and 3.2 Jy respectively at 87.9 GHz in Kuan et al. (1996), although Kuan et al. do find that N has a very steep spectrum (spectral index  $\alpha = 4.6 \pm 0.5$ , where  $S_\nu \propto \nu^\alpha$  so that the flux ratio is steeply frequency dependent). The positions from the ATCA 2003 continuum data are (J2000) 17 47 20.07, -28 22 18.2 for N and 17 47 20.39, -28 22 13.4 for N'. Due to the self-calibration applied, the absolute positions may be somewhat uncertain, but the relative offset of N', 4.3 arcsec east and 4.7 arcsec north of N, is more reliable.

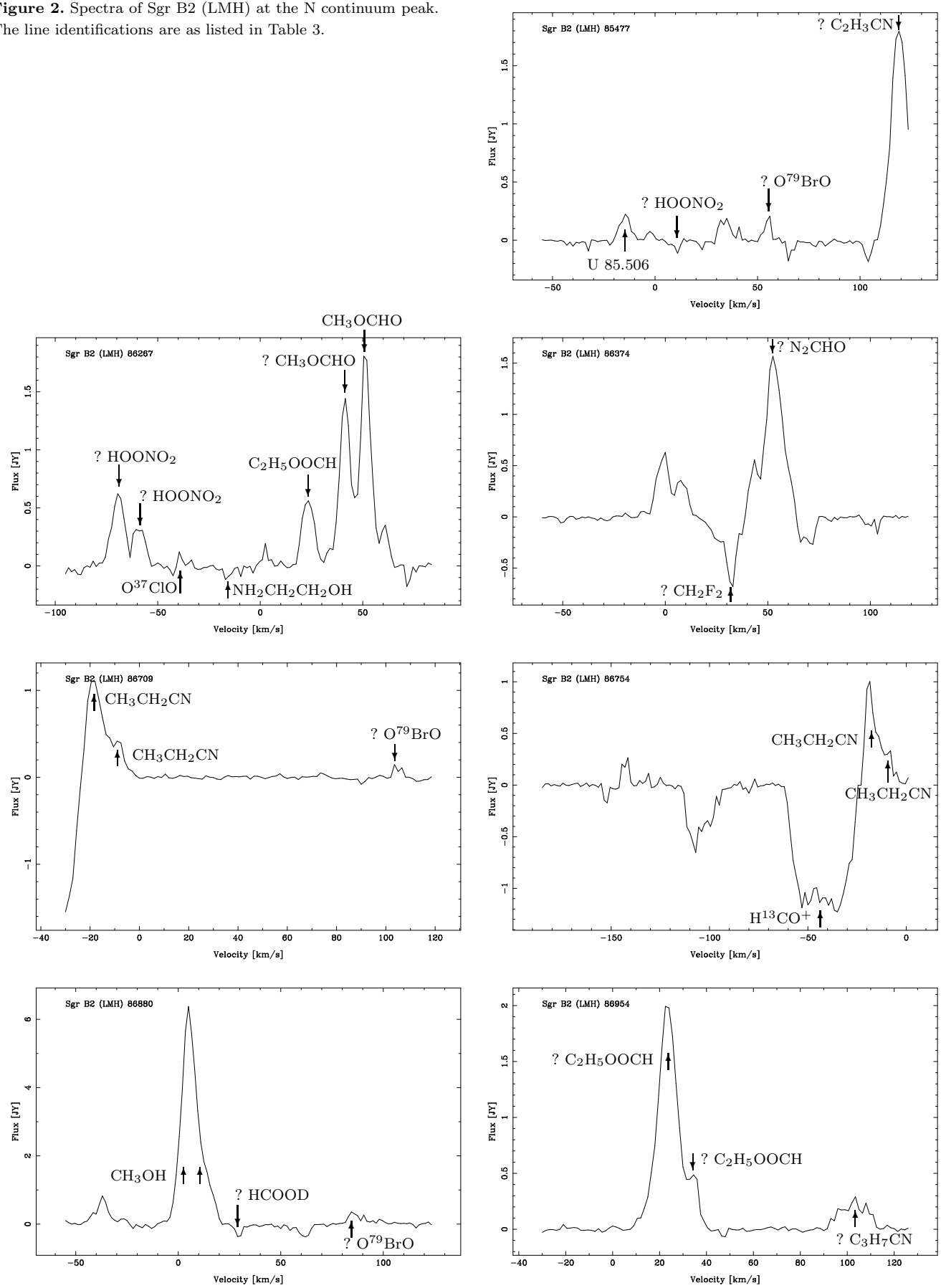
### 3.2 Sgr B2 line emission and absorption

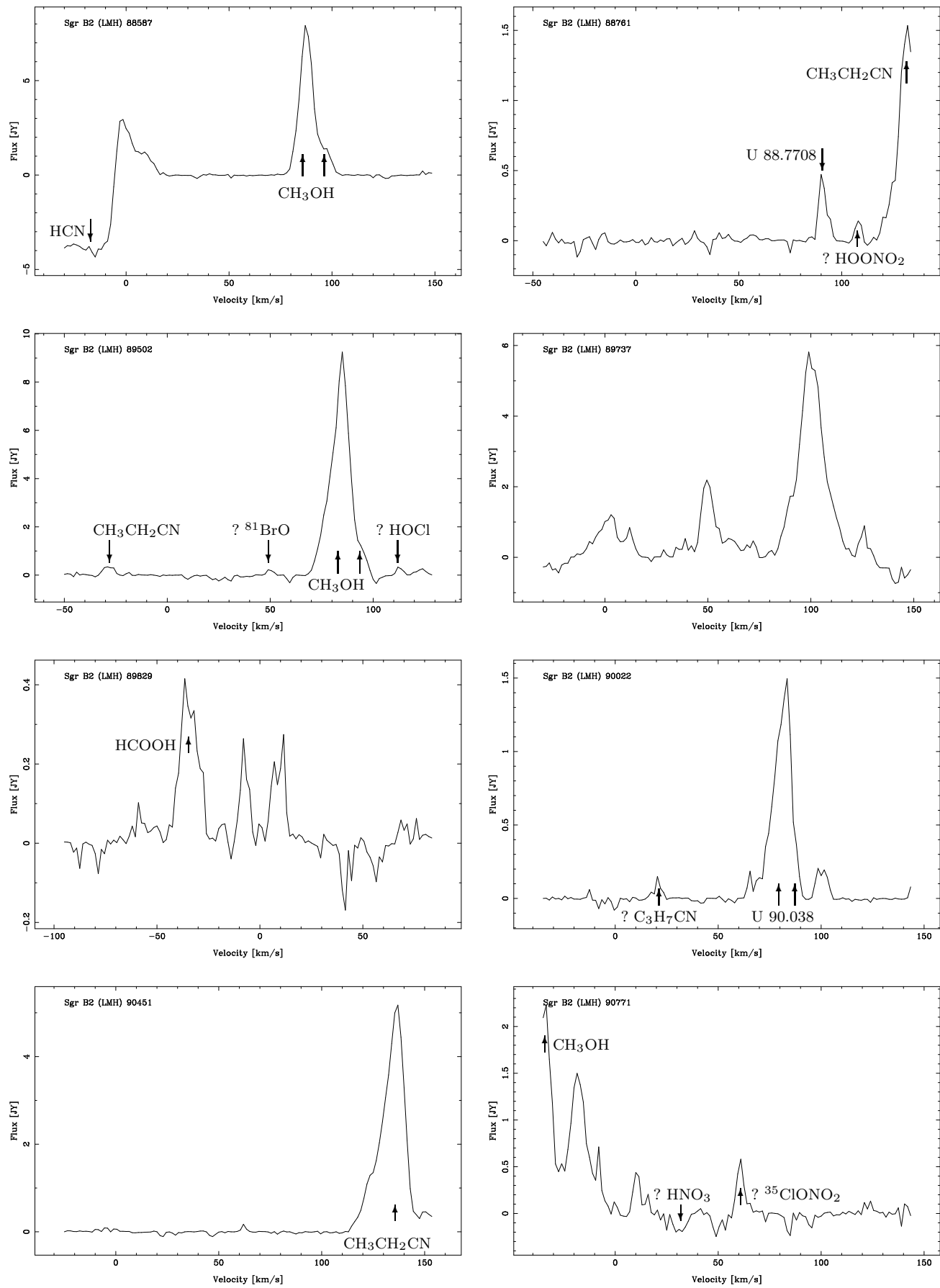
The ATCA data cubes for Sgr B2 showed many line emission and absorption features. These features were spatially located close to the continuum position N, so for display in figure 2 we show the spectra at the pixel close to the N peak (0.5 arcsec west and 0.2 arcsec north of the fitted N continuum position above).

The RMS noise ( $\sigma$ ) levels in the data cubes, obtained after clipping pixels at the  $3\sigma$  level to reduce bias, are given in table 2. The values are in the range 14 to 35 mJy/beam, which is in good agreement with the expected thermal noise given the ATCA instrumental parameters (User's Guide to 3-mm Observing with the ATCA, <http://www.atnf.csiro.au/observers/docs/3mm/index.html>) and the integration time for the data sets. Spectral-line features in the data cubes were considered significant at the  $5\sigma$  level. Note that there are strong emission features (up to 8 Jy/beam in band labelled 89502), but also strong absorption features, such as that at -43 km/s in the band labelled 86754, which is identified with  $\text{H}^{13}\text{CO}^+$ . The continuum brightness temperature of component N is around 60 K, using the integrated flux 4.7 Jy, and deconvolved HPBW of 4.3 arcsec  $\times$  2.9 arcsec from the 2003 data, although somewhat uncertain due to the uncertainty in the deconvolved source size. As line absorption can occur if the line excitation temperature is less than this background brightness temperature, we consider both line absorption and emission features at the continuum peaks.

The line features in the data cubes were fitted as Gaussians, using the MIRIAD task *gaufit*, at a pixel near the N continuum position (0.5 arcsec west and 0.8 arcsec south) where the line emission and absorption was centred. The peak flux (Jy), width (km/s) and integrated flux (Jy km/s) are quoted in table 3. To enable comparison with the plots in figure 2, and since the data cubes have velocity axes, the fitted line position is given as both a velocity and a frequency.

**Figure 2.** Spectra of Sgr B2 (LMH) at the N continuum peak. The line identifications are as listed in Table 3.





The conversion of fitted line velocities to rest frequency requires the appropriate radial velocity for the emitting region - this is not trivial because of the multiple velocity components in Sgr B2. Lines previously detected in the interstellar medium were identified from the NIST on-line database of Lovas (<http://physics.nist.gov/PhysRefData/Micro/Html/contents.html>), and given in the last column of table 3. For five known lines where the emission is peaked near continuum position N, this gives radial velocity 63.5 km/s (with standard deviation 0.7 km/s). For some of the strong lines in the data cubes, there is a second component seen 5 arcsec north of the other lines (0.5 arcsec west and 4.2 arcsec north of the N continuum). These lines, labelled d (for double lines) in the Identification column of table 3, were refitted in the data cubes at this more northern position. For the same five known lines from the NIST database, these give radial velocity 73.1 km/s (standard deviation 0.4 km/s) for this position. The rest frequencies quoted in table 3 were therefore calculated assuming radial velocity 63.5 km/s for the position near the N continuum, and 73.1 km/s for the more northerly position, labelled d in table 3. This spatial and velocity structure is similar to that found by Hollis et al. (2003b) in VLA observations of ethyl cyanide at 43.5 GHz, and other previous observations of Sgr B2 (LMH).

We list, in table 3, 58 emission features and 21 absorption features significant at the  $5\sigma$  level in the 15 chunks of spectrum searched. Assuming 50 MHz for each band (dropping the edges of the original 64 MHz bands), this gives around 75 emission features per GHz and 25 absorption features per GHz stronger than the median  $5\sigma$  level of 110 mJy, after making small corrections for the incompleteness above the 110 mJy level, and the double-counting of the emission line at 86.745 GHz in the overlap between the 86709 and 87754 bands. This is slightly higher than the line density of 61 per GHz in the survey of Friedel et al (2004) from BIMA and NRAO 12-m observations of Sgr B2 (N-LMH), although we have not covered as large a frequency range. Given the median line width of 6.5 km/s, corresponding to a width of 1.9 MHz, we find that the spectra have reached a level where there is line confusion, with around 1/5 of the band covered with lines. The number of emission features varies with flux density as  $n(> S) \propto S^{-0.5}$  and absorption features as  $n(> S) \propto S^{-1.0}$ .

## 4 DISCUSSION

The lines detected (figure 3.2 and table 3) were checked against line frequencies from the Jet Propulsion Laboratory (JPL, Pickett et al. 1998) and Cologne Database for Molecular Spectroscopy (CDMS, Müller et al 2001) on-line databases. We list in table 3 several lines, with identifications marked L, where the lines have previously been detected and listed in the NIST database of Lovas. We are confident of these identifications. We also list in table 3, possible identifications based on the JPL on-line database, marked with ? and J. These correspond to listed transitions within 0.5 MHz (around 1.7 km/s) of our measured frequencies (using velocity 63.5 km/s for the main component of Sgr B2 LMH), where the listed frequency uncertainty is less than 0.5 MHz. Due to the large number of transitions listed in the

JPL database, we have excluded some line identifications with weak transitions which would imply implausibly high total column densities (below), and which therefore should have been detected in stronger transitions in other line surveys. We have made 27 tentative assignments in table 3, but many of these involve molecules not previously detected in the ISM, and cannot be regarded with confidence. Observations of other transitions of these molecules are now necessary to confirm or exclude a detection.

Using standard assumptions of LTE radiative transfer (eg. Rolfs & Wilson 2004) the column density  $N_u$  of molecules in the upper level of the transition is related to the line intensity by

$$N_u = (8\pi\nu^2 k / hc^3 A_{ul}) \int T_B dv$$

where  $A_{ul}$  is the Einstein coefficient, and  $\int T_B dv$  is the integral over velocity of the brightness temperature  $T_B$  of the emission line. The Einstein coefficients  $A_{ul}$  were obtained from the Pickett JPL or CDMS on-line databases from the tabulated log of intensity  $I(T_o)$  at reference temperature  $T_o = 300$  K. For some species (CH<sub>3</sub>OH below) CDMS tabulated values of the log of  $S_g \mu_g^2$  are given, and were used to calculate  $A_{ul}$ .

The total column density  $N$  of the molecule is given by

$$N = (N_u / g_u) Q_T \exp(E_u / kT_{ex})$$

where  $Q_T$  is the partition function at excitation temperature  $T_{ex}$ ,  $E_u$  is the energy of the upper level and  $g_u$  is the statistical weight of the upper level. Values for  $g_u$ , the lower state energy  $E_l$ , frequency  $\nu$  and  $Q$  as a function of temperature were obtained from the JPL database. If several transitions of the same molecule are observed (with different upper levels) then this relation can be used, as below in a “rotation diagram”, to determine both  $N$  and  $T_{ex}$ .

We did not confidently detect either the glycine or propylene oxide lines. We can set  $3\sigma$  upper limits for most of the lines searched. Due to the large number of confusing absorption and emission lines, there are several observed spectral features that lie close to the lines searched, but not close enough to be line identifications. We judge that the absorption lines are unlikely to be propylene oxide or glycine identifications, since absorption would be due to quite cold dense gas, and that very strong emission lines are unlikely to be identifications, as they would be inconsistent with the upper limits given by other transitions not detected.

### 4.1 Upper limits for glycine

For glycine, conformers I and II, we use the molecular parameters from the JPL database to calculate the upper limits for the column density of the upper level of the transition  $N_u$ , and the total column density  $N$ . The results are given in table 4. Since there are several hyperfine components blended together for each line, with different Einstein coefficients  $A_{ul}$  and statistical weights  $g_u$ , we quote  $N_u$  based on the main level, with  $A_{ul}$  and  $g_u$  for this level. We include all of the hyperfine components in the calculation for  $N$ , by considering  $\sum A_{ul} g_u$  for all the components. We have assumed excitation temperature  $T_{ex} = 75$  K, as estimated by Kuan et al. (2003) for glycine I in Sgr B2 (LMH), and  $Q(75) = 29377$  for both conformers.

**Table 3.** Emission and absorption lines detected above the  $5\sigma$  level. Most are spatially associated with the 64 km/s cloud, and we assumed a cloud velocity of 63.5 km/s to convert the observed frequency to rest frequency, whereas lines marked ‘d’ are associated with the 73 km/s cloud and assume a velocity of 73.1 km/s.

| Band Label | Frequency (GHz) | Velocity (km/s) | Peak (Jy) | Width (km/s) | Integrated (Jy km/s) | Identification  |
|------------|-----------------|-----------------|-----------|--------------|----------------------|---|
| 85477      | 85.4683         | 119.1           | 1.84      | 9.1          | 17.8                 | ? C <sub>2</sub> H <sub>3</sub> CN 85.46862 J                   |
|            | 85.4727         | 103.7           | -0.149    | (5)          | -0.79                |   |
|            | 85.4836         | 65.7            | -0.149    | 3.6          | -0.57                |   |
|            | 85.4866         | 55.2            | 0.219     | 3.0          | 0.70                 | ? O <sup>79</sup> BrO 85.48633 J                                |
|            | 85.4926         | 34.1            | 0.180     | 6.3          | 1.21                 |   |
|            | 85.4993         | 10.6            | -0.097    | 3.7          | -0.38                | ? HOONO <sub>2</sub> 85.49896 J                                 |
|            | 85.5064         | -14.2           | 0.144     | 10.8         | 1.66                 | U 85.506 L  |
| 86267      | 86.2597         | 72.4            | -0.115    | (5)          | -0.61                |   |
|            | 86.2631         | 60.5            | 0.34      | 5.1          | 1.84                 |   |
|            | 86.2657         | 51.4            | 1.83      | 5.9          | 11.5                 | CH <sub>3</sub> OCHO 86.265826 L                                |
|            | 86.2686         | 41.4            | 1.43      | 6.3          | 9.6                  | ? CH <sub>3</sub> OCHO 86.26865 J                               |
|            | 86.2738         | 23.4            | 0.59      | 6.9          | 4.3                  | ? C <sub>2</sub> H <sub>5</sub> OOCH 86.27379 J                 |
|            | 86.2798         | 2.5             | 0.198     | 2.0          | 0.42                 |   |
|            | 86.2850         | -15.5           | -0.078    | 9.0          | -0.75                | ? NH <sub>2</sub> CH <sub>2</sub> CH <sub>2</sub> OH 86.28495 J |
|            | 86.2918         | -39.0           | 0.173     | 1.5          | 0.276                | ? O <sup>37</sup> ClO 86.29165 J                                |
|            | 86.3002         | -58.4           | 0.57      | (8)          | 4.9                  | d ? HOONO <sub>2</sub> 86.30031 J                               |
|            | 86.3005         | -69.1           | 0.65      | 8.4          | 5.8                  | ? HOONO <sub>2</sub> 86.30031 J                                 |
| 86374      | 86.3691         | 101.3           | -0.095    | 7.2          | -0.73                |   |
|            | 86.3782         | 69.7            | -0.284    | 6.5          | -1.97                |   |
|            | 86.3831         | 52.9            | 1.45      | 11.0         | 17.0                 | ? N <sub>2</sub> CHO 86.38325 J                                 |
|            | 86.3892         | 31.7            | -0.61     | 7.3          | -4.7                 | ? CH <sub>2</sub> F <sub>2</sub> 86.38924 J                     |
|            | 86.3986         | 8.6             | 0.73      | 5.1          | 4.0                  | d   |
|            | 86.3986         | -0.8            | 0.62      | 9.3          | 6.2                  |   |
| 86709      | 86.7097         | 104.7           | 0.118     | 4.2          | 0.53                 | ? O <sup>79</sup> BrO 86.70978 J                                |
|            | 86.7453         | -8.7            | 0.94      | 5.1          | 5.1                  | d CH <sub>3</sub> CH <sub>2</sub> CN 86.745317 L                |
|            | 86.7453         | -18.1           | 1.78      | 6.7          | 12.7                 | CH <sub>3</sub> CH <sub>2</sub> CN 86.745317 L                  |
| 86754      | 86.7454         | -9.1            | 0.77      | 5.2          | 4.3                  | d CH <sub>3</sub> CH <sub>2</sub> CN 86.745317 L                |
|            | 86.7454         | -18.5           | 1.10      | 9.3          | 10.9                 | CH <sub>3</sub> CH <sub>2</sub> CN 86.745317 L                  |
|            | 86.7526         | -43.3           | -1.34     | 23.8         | -33                  | H <sup>13</sup> CO <sup>+</sup> 86.754330 L                     |
|            | 86.7706         | -105.4          | -0.54     | 13.1         | -7.5                 |   |
|            | 86.7814         | -142.6          | 0.252     | 3.8          | 1.02                 |   |
|            | 86.7843         | -152.6          | -0.230    | 2.1          | -0.51                |   |
| 86880      | 86.8793         | 86.4            | 0.288     | 9.0          | 2.76                 | ? O <sup>79</sup> BrO 86.8799 J                                 |
|            | 86.8866         | 61.2            | -0.36     | 7.0          | -2.71                |   |
|            | 86.8958         | 29.6            | -0.40     | 3.6          | -1.52                | ? HCOOD 86.89546 J  |
|            | 86.9031         | 14.0            | 2.12      | 7.8          | 17.6                 | d CH <sub>3</sub> OH 86.902947 L                                |
|            | 86.9029         | 5.2             | 6.6       | 5.2          | 36                   | CH <sub>3</sub> OH 86.902947 L                                  |
|            | 86.9150         | -26.9           | 0.42      | 4.5          | 2.01                 | d   |
|            | 86.9152         | -37.1           | 0.81      | 6.9          | 5.9                  |   |
| 86954      | 86.9556         | 102.8           | 0.235     | 14.1         | 3.5                  | ? C <sub>3</sub> H <sub>7</sub> CN 86.95546 J                   |
|            | 86.9784         | 34.1            | 0.99      | 5.3          | 5.6                  | d ? C <sub>2</sub> H <sub>5</sub> OOCH 86.97838 J               |
|            | 86.9787         | 23.3            | 2.09      | 9.4          | 20.9                 | ? C <sub>2</sub> H <sub>5</sub> OOCH 86.97838 J                 |
| 88587      | 88.5948         | 97.4            | 2.93      | 6.3          | 19.7                 | d CH <sub>3</sub> OH 88.594809 L                                |
|            | 88.5946         | 88.3            | 7.5       | 7.5          | 60                   | CH <sub>3</sub> OH 88.594809 L                                  |
|            | 88.6191         | 5.8             | 2.78      | 14.9         | 44                   |   |
|            | 88.6215         | -2.3            | 4.5       | 6.8          | 33                   |   |
|            | 88.6263         | -18.5           | -4.2      | 41.3         | -183                 | HCN 88.6304157 L  |
| 88761      | 88.7583         | 132.2           | 1.47      | 10.6         | 16.6                 | CH <sub>3</sub> CH <sub>2</sub> CN 88.758419 L                  |
|            | 88.7655         | 108.1           | 0.151     | 3.3          | 0.53                 | ? HOONO <sub>2</sub> 88.76542 J                                 |
|            | 88.7706         | 90.7            | 0.45      | 4.5          | 2.17                 | U 88.7708 L   |

| Band Label | Frequency (GHz) | Velocity (km/s) | Peak (Jy) | Width (km/s) | Integrated (Jy km/s) | Identification  |
|------------|-----------------|-----------------|-----------|--------------|----------------------|---|
| 89502      | 89.4946         | 122.3           | 0.188     | (9.6)        | 1.92                 | ? HOCl 89.49483 J   |
|            | 89.4974         | 113.1           | 0.227     | (6.4)        | 1.55                 |   |
|            | 89.5003         | 103.2           | -0.158    | (6.4)        | -1.08                |   |
|            | 89.5056         | 95.1            | 2.38      | 5.1          | 12.9                 | d CH <sub>3</sub> OH 89.505778 L<br>CH <sub>3</sub> OH 89.505778 L          |
|            | 89.5061         | 83.8            | 8.3       | 10.7         | 95                   |   |
|            | 89.5134         | 59.6            | -0.162    | (6.4)        | -1.10                |   |
|            | 89.5162         | 50.0            | 0.125     | (8)          | 1.07                 |   |
|            | 89.5232         | 26.6            | -0.178    | 14.8         | -2.81                |   |
|            | 89.5397         | -28.5           | 0.38      | 5.7          | 2.28                 |   |
| 89737      | 89.7319         | 125.5           | 0.80      | 8.3          | 7.1                  |   |
|            | 89.7395         | 100.2           | 5.4       | 14.7         | 84                   |   |
|            | 89.7546         | 50.1            | 2.06      | 8.3          | 18.2                 |   |
|            | 89.7688         | 2.6             | 0.99      | 16.5         | 17.4                 |   |
| 89829      | 89.8482         | 9.2             | 0.216     | 7.9          | 1.82                 |   |
|            | 89.8532         | -7.6            | 0.235     | 4.7          | 1.18                 |   |
|            | 89.8613         | -34.5           | 0.35      | (12)         | 4.5                  | HCOOH 89.86148 L  |
| 90022      | 90.0320         | 100.3           | 0.207     | 6.1          | 1.35                 |   |
|            | 90.0375         | 91.8            | 0.33      | 14.6         | 5.1                  | d U 90.038 L<br>U 90.038 L<br>? C <sub>3</sub> H <sub>7</sub> CN 90.05591 J |
|            | 90.0378         | 81.1            | 0.97      | 9.8          | 10.1                 |   |
|            | 90.0560         | 20.8            | 0.138     | 2.9          | 0.43                 |   |
| 90451      | 90.4535         | 135.1           | 4.7       | 13.0         | 65                   | CH <sub>3</sub> CH <sub>2</sub> CN 90.453354 L                              |
| 90771      | 90.7740         | 94.9            | -0.164    | 2.9          | -0.51                |   |
|            | 90.7772         | 84.4            | -0.30     | 2.1          | -0.67                |   |
|            | 90.7844         | 60.8            | 0.58      | 3.8          | 2.33                 | ? <sup>35</sup> ClONO <sub>2</sub> 90.78419 J                               |
|            | 90.7877         | 49.8            | -0.194    | 6.1          | -1.26                |   |
|            | 90.7935         | 30.8            | -0.190    | 8.4          | -1.70                |   |
|            | 90.7996         | 10.5            | 0.47      | 3.7          | 1.84                 |   |
|            | 90.8083         | -17.9           | 1.32      | 12.1         | 17.0                 |   |
|            | 90.8132         | -34.1           | 2.21      | 6.9          | 16.2                 | CH <sub>3</sub> OH 90.81239 L   |

The conformer II is higher in energy than conformer I by  $W_c = 705 \text{ cm}^{-1}$  (energy expressed as  $1/\lambda = E/hc$ ) Lovas et al. (1995) with uncertainty 10 %, or  $E/k = 1014 \pm 100 \text{ K}$ . The energy levels of glycine II are expressed relative to the lowest energy state of glycine I in the JPL database and table 4, but we have considered the two conformers as separate species in the total column density calculations. Hence when correcting for the Maxwell-Boltzmann distribution of levels we converted the energies to those relative to the lowest energy state of glycine II for the  $\exp(E_u/kT_{ex})$  factor, to match the usage in the partition function. The column density limits obtained for conformer II of glycine are considerably tighter than those of conformer I due to its larger dipole moment.

The column density limits are averaged over the synthesised beam, and are derived from the brightness temperature limits, so they depend on the beam size. The best upper limit for glycine I from these ATCA observations is  $N = 1.4 \times 10^{15} \text{ cm}^{-2}$  with the beam size of  $17.0 \times 3.4 \text{ arcsec}^2$ . If the glycine emission is indeed extended over a scale larger than the beam, then this non-detection is consistent with the value of  $N = 4 \times 10^{14} \text{ cm}^{-2}$  obtained in Sgr B2 LMH by Kuan et al. (2003) with the NRAO 12-m.

However, if glycine were confined to the scale of the LMH continuum source ( $< 5 \text{ arcsec}$ ), then the column den-

sities calculated would be beam diluted, and diluted differently by the different beam sizes. Assuming beam size 30 arcsec for the NRAO 12-m at 1.3 mm, the beam area ratio is  $(30 \times 30)/(17 \times 3.4) = 15.6$ , so that the ratio of ATCA/NRAO 12-m column density of  $< 14/4$  or  $< 3.5$  would be  $< 0.22$  when corrected for a small scale of glycine emission. In other words, if the glycine calculated at a column density of  $N = 4 \times 10^{14} \text{ cm}^{-2}$  by Kuan et al. (2003) was distributed over the scale of a few arcsec (as, for example, methyl formate and acetic acid are) we would have easily detected it in these ATCA observations. We therefore conclude that the ATCA upper limit provides a strong limit on any small-scale glycine emission, for both of conformers I and II.

#### 4.2 Upper limits for propylene oxide

We have also calculated the upper limits for the column density of propylene oxide (table 4). We have assumed excitation temperature  $T_{ex} = 200 \text{ K}$ , as typical for Sgr B2 (LMH) as determined by other species (see below section 4.3), and  $Q(200) = 17811$  from the the approximate formula  $Q(T) = (kT/h)^{3/2}(\pi/ABC)^{1/2}$  and the rotational constants A,B,C from Creswell & Schwendeman (1977). The energy levels and Einstein coefficients (table 4) were calculated with

**Table 4.** Column density upper limits for glycine and propylene oxide lines searched, at the  $3\sigma$  level, for those lines which were not confused. We label with ‘conf.’ the transitions which were confused, and give the frequency of the confusing lines. We list flux density and brightness temperature limits, molecular line parameters  $A_{ul}$ ,  $g_u$ ,  $E_u/k$ , and column density limits for the upper level of the transition  $N_u$  and the total  $N$ . The calculations have been made assuming that the distribution of the molecules is extended with respect to the ATCA synthesized beam size of  $17.0 \times 3.4$  arcsec $^2$ .

| Line Freq.<br>(GHz) | ID   | Transition                              | Limit<br>(mJy) | Limit<br>(K) | $A_{ul}$<br>(s $^{-1}$ ) | $g_u$ | $E_u/k$<br>(K) | $N_u$<br>(cm $^{-2}$ ) | $N$<br>(cm $^{-2}$ ) |
|---------------------|------|---|----------------|--------------|--------------------------|-------|----------------|------------------------|----------------------|
| 89.51220            | G I  | 13 <sub>6,8</sub> – 12 <sub>6,7</sub>   | 78             | 0.37         | $2.65 \times 10^{-6}$    | 81    | 41.9           | $1.5 \times 10^{13}$   | $4.7 \times 10^{15}$ |
| 89.53550            | G I  | 13 <sub>6,7</sub> – 12 <sub>6,6</sub>   | 78             | 0.37         | $2.65 \times 10^{-6}$    | 81    | 41.9           | $1.5 \times 10^{13}$   | $4.7 \times 10^{15}$ |
| 89.83184            | G I  | 14 <sub>1,13</sub> – 13 <sub>1,12</sub> | 78             | 0.20         | $3.29 \times 10^{-6}$    | 87    | 34.4           | $6.8 \times 10^{12}$   | $1.8 \times 10^{15}$ |
| 89.87571            | G I  | 13 <sub>5,9</sub> – 12 <sub>5,8</sub>   | 78             | 0.20         | $2.90 \times 10^{-6}$    | 81    | 38.3           | $7.7 \times 10^{12}$   | $2.3 \times 10^{15}$ |
| 90.04967            | G I  | 15 <sub>0,15</sub> – 14 <sub>0,14</sub> | 66             | 0.17         | $3.40 \times 10^{-6}$    | 93    | 35.4           | $5.5 \times 10^{12}$   | $1.4 \times 10^{15}$ |
| 86.262231           | G II | 12 <sub>6,7</sub> – 11 <sub>6,6</sub>   | 48             | 0.24         | $7.8 \times 10^{-5}$     | 75    | 1044.7         | $3.1 \times 10^{11}$   | $1.0 \times 10^{14}$ |
| 86.283667           | G II | 12 <sub>6,6</sub> – 11 <sub>6,5</sub>   | 48             | 0.24         | $7.8 \times 10^{-5}$     | 75    | 1044.7         | $3.1 \times 10^{11}$   | $1.0 \times 10^{14}$ |
| 86.716051           | G II | 13 <sub>1,12</sub> – 12 <sub>1,11</sub> | 42             | 0.33         | $1.0 \times 10^{-4}$     | 81    | 1037.7         | $3.2 \times 10^{11}$   | $8.9 \times 10^{13}$ |
| 86.960812           | G II | 14 <sub>1,14</sub> – 13 <sub>1,13</sub> | 45             | 0.35         | $1.1 \times 10^{-4}$     | 87    | 1038.7         | $3.3 \times 10^{11}$   | $8.6 \times 10^{13}$ |
| 86.967057           | G II | 14 <sub>0,14</sub> – 13 <sub>0,13</sub> | 45             | 0.35         | $1.1 \times 10^{-4}$     | 87    | 1038.7         | $3.3 \times 10^{11}$   | $8.6 \times 10^{13}$ |
| 88.792618           | G II | 6 <sub>4,2</sub> – 5 <sub>3,3</sub>     | 99             | 0.27         | $1.9 \times 10^{-6}$     | 39    | 1018.8         | $1.5 \times 10^{13}$   | $6.7 \times 10^{15}$ |
| 86.72160            | PO   | 7 <sub>0,7</sub> – 6 <sub>0,6</sub>     | 42             | 0.33         | $3.17 \times 10^{-6}$    | 15    | 16.8           | $1.0 \times 10^{13}$   | $1.3 \times 10^{16}$ |
| 88.59909            | PO   | 7 <sub>4,4</sub> – 6 <sub>4,3</sub>     | 105            | 0.50         | $2.30 \times 10^{-6}$    | 15    | 25.9           | $2.3 \times 10^{13}$   | $3.1 \times 10^{16}$ |
| 88.60199            | PO   | 7 <sub>4,3</sub> – 6 <sub>4,2</sub>     | 105            | 0.50         | $2.30 \times 10^{-6}$    | 15    | 25.9           | $2.3 \times 10^{13}$   | $3.1 \times 10^{16}$ |
| 88.77871            | PO   | 7 <sub>3,4</sub> – 6 <sub>3,3</sub>     | 99             | 0.27         | $2.80 \times 10^{-6}$    | 15    | 22.0           | $1.0 \times 10^{13}$   | $1.3 \times 10^{16}$ |
| 89.87218            | PO   | 7 <sub>2,5</sub> – 6 <sub>2,4</sub>     | 78             | 0.20         | $3.27 \times 10^{-6}$    | 15    | 19.4           | $6.8 \times 10^{12}$   | $8.9 \times 10^{15}$ |
| 90.47516            | PO   | 7 <sub>1,6</sub> – 6 <sub>1,5</sub>     | 93             | 0.24         | $3.55 \times 10^{-6}$    | 15    | 17.9           | $7.5 \times 10^{12}$   | $9.7 \times 10^{15}$ |
| 86.88593            | G I  | 12 <sub>3,9</sub> – 11 <sub>3,8</sub>   | conf.          | 86.8866 abs. |                          |       |                |                        |                      |
| 89.50043            | G I  | 14 <sub>2,13</sub> – 13 <sub>2,12</sub> | conf.          | 89.5003 abs. |                          |       |                |                        |                      |
| 89.75055            | G I  | 13 <sub>4,10</sub> – 12 <sub>4,9</sub>  | conf.          | 89.7546 em.  |                          |       |                |                        |                      |
| 90.03589            | G I  | 15 <sub>0,15</sub> – 14 <sub>1,14</sub> | conf.          | 90.0378 em.  |                          |       |                |                        |                      |
| 90.04311            | G I  | 15 <sub>1,15</sub> – 14 <sub>1,14</sub> | conf.          | 90.0378 em.  |                          |       |                |                        |                      |
| 90.05689            | G I  | 15 <sub>0,15</sub> – 14 <sub>0,14</sub> | conf.          | 90.0560 em.  |                          |       |                |                        |                      |
| 90.78355            | G I  | 13 <sub>2,11</sub> – 12 <sub>2,10</sub> | conf.          | 90.7844 em.  |                          |       |                |                        |                      |
| 86.379992           | G II | 13 <sub>2,12</sub> – 12 <sub>2,11</sub> | conf.          | 86.3782 abs. |                          |       |                |                        |                      |
| 86.978582           | G II | 12 <sub>5,7</sub> – 11 <sub>5,6</sub>   | conf.          | 86.9787 em.  |                          |       |                |                        |                      |
| 85.48422            | PO   | 7 <sub>1,7</sub> – 6 <sub>1,6</sub>     | conf.          | 85.4836 abs. |                          |       |                |                        |                      |

a rigid asymmetric rotor model, using the spectroscopic constants from Creswell & Schwendeman (1977) and the dipole moment components from Swalen & Herschbach (1957).

#### 4.3 Ethyl cyanide and methanol

Due to the large number of strong transitions of ethyl cyanide ( $\text{CH}_3\text{CH}_2\text{CN}$ ) and methanol ( $\text{CH}_3\text{OH}$ ) in the 3-mm band, we have measured serendipitously 4 transitions of each molecule. These two molecules are found in the small scale structure near continuum source N, at around 64 km/s, and also found at the other component at 73 km/s 5 arcsec to the north. To calculate the brightness temperature and column density, we assume a size  $3.5 \times 2.0$  arcsec, based on the median spatial size of line emission in our datacubes. The upper level column densities are given in table 5, along with some of the molecular parameters used.

Given the detection of several transitions at different upper energy levels, we can fit rotation diagrams to derive the excitation temperature and total column density. The fits give  $T_{ex} = 175$  K and  $N = 8.4 \times 10^{17}$  cm $^{-2}$  for

$\text{CH}_3\text{CH}_2\text{CN}$  in the main 64 km/s cloud,  $T_{ex} = 190$  K and  $N = 1.1 \times 10^{19}$  cm $^{-2}$  for  $\text{CH}_3\text{OH}$  in the 64 km/s cloud and  $T_{ex} = 220$  K and  $N = 3.4 \times 10^{18}$  cm $^{-2}$  for  $\text{CH}_3\text{OH}$  in the 73 km/s cloud.

These excitation temperatures are in good agreement with that expected for Sgr B2 LMH, eg. 170 K for  $\text{CH}_3\text{OH}$  from Pei, Liu & Snyder (2000). The estimates of column density are dependent on the assumed source size, but our estimate of total column density for  $\text{CH}_3\text{CH}_2\text{CN}$  in Sgr B2 LMH is about a factor of two higher than that obtained by Miao & Snyder (1997), Liu & Snyder (1999) and Liu, Mehringer & Snyder (2001) when corrected for the different assumed sizes. Similarly, our estimate of column density for  $\text{CH}_3\text{OH}$  is in good agreement (30 % higher) with that of Pei et al. (2000) when corrected for source size.

#### 5 CONCLUSIONS

We have used the ATCA during 2002 and 2003 to conduct a search for the simplest amino acid, glycine, and the simple chiral molecule propylene oxide, at 3-mm, using the

**Table 5.** Methanol and ethyl cyanide results.

| ID and Freq.<br>(GHz)                 | Transition                                | $A_{ul}$<br>(s $^{-1}$ ) | $g_u$ | $E_u/k$<br>(K) | $N_u$<br>(cm $^{-2}$ )<br>64 km/s | $N_u$<br>(cm $^{-2}$ )<br>73 km/s |
|---------------------------------------|---|--------------------------|-------|----------------|-----------------------------------|-----------------------------------|
| <b>CH<sub>3</sub>OH</b>               |   |                          |       |                |                                   |                                   |
| 86.902947                             | 7 <sub>2,5</sub> – 6 <sub>3,4</sub>       | $6.85 \times 10^{-7}$    | 15    | 102.7          | $1.8 \times 10^{16}$              | $8.6 \times 10^{15}$              |
| 88.594809                             | 15 <sub>3,13</sub> – 14 <sub>4,10</sub>   | $1.10 \times 10^{-6}$    | 31    | 338.1          | $1.9 \times 10^{16}$              | $6.1 \times 10^{15}$              |
| 89.505778                             | 8 <sub>–4,5</sub> – 9 <sub>–3,7</sub>     | $7.65 \times 10^{-7}$    | 17    | 171.4          | $4.2 \times 10^{16}$              | $5.7 \times 10^{15}$              |
| 90.81239                              | 20 <sub>–3,17</sub> – 19 <sub>–2,17</sub> | $2.81 \times 10^{-6}$    | 41    | 807.9          | $2.0 \times 10^{15}$              |                                   |
| <b>CH<sub>3</sub>CH<sub>2</sub>CN</b> |   |                          |       |                |                                   |                                   |
| 86.745317                             | 8 <sub>1,8</sub> – 7 <sub>0,7</sub>       | $3.39 \times 10^{-6}$    | 17    | 16.1           | $1.2 \times 10^{15}$              | $4.7 \times 10^{14}$              |
| 88.758419                             | 27 <sub>3,24</sub> – 27 <sub>2,25</sub>   | $4.89 \times 10^{-6}$    | 55    | 174.0          | $1.2 \times 10^{15}$              |                                   |
| 89.53945                              | 33 <sub>4,30</sub> – 32 <sub>5,27</sub>   | $1.01 \times 10^{-6}$    | 67    | 259.4          | $7.6 \times 10^{14}$              |                                   |
| 90.453354                             | 10 <sub>2,8</sub> – 9 <sub>2,7</sub>      | $5.88 \times 10^{-5}$    | 21    | 28.2           | $3.8 \times 10^{14}$              |                                   |

three millimetre capable antennas available at that time. We searched 15 portions of spectrum between 85 and 91 GHz, each of 64 MHz bandwidth. The main results are as follows:

- We have detected 58 emission features and 21 absorption features in the 15 portions of spectrum searched. This gives a line density of 75 emission and 25 absorption lines per GHz stronger than the  $5\sigma$  level of 110 mJy.
- We have tentatively assigned 23 of the detected spectral lines to transitions listed in the JPL on-line database (table 3) but as many of these involve molecules not previously detected in the ISM, these assignments cannot be regarded with confidence.
- We did not confidently detect either glycine or propylene oxide, but can set  $3\sigma$  upper limits for most transitions searched.
- Assuming that the glycine emission is extended with respect to the ATCA synthesised beam size of  $17.0 \times 3.4$  arcsec $^2$ , our  $3\sigma$  upper limit of  $N = 1.4 \times 10^{15}$  cm $^{-2}$  is consistent with that of  $N = 4 \times 10^{14}$  cm $^{-2}$  of Kuan et al. (2003) in their reported detection of glycine. However, at the column density reported by Kuan et al. (2003) we show that if glycine were confined to the scale of the LMH continuum source ( $< 5$  arcsec), it would have been easily detected in these ATCA observations. These ATCA observations therefore put a strong upper limit on any small-scale glycine emission in Sgr B2, for both of conformers I and II.

## ACKNOWLEDGMENTS

The Monash authors acknowledge the financial support provided by the Australia Telescope National Facility for the construction of the laboratory spectrometer, the spectrometer design, construction and technical services provided by Jonathan G. Crofts, and the collaboration with Takeshi Sakaizumi in the laboratory measurements of the Glycine spectrum. PAJ would like to acknowledge the support provided by an Australia Telescope National Facility Visiting Fellowship. We also thank the referee for very useful comments that improved the clarity and presentation of the paper.

## REFERENCES

Bailey J., Chrysostomou A., Hough J.H., Gledhill T.M., McCall A., Clark S., Menard F., Tamura M. 1998. *Science* 281, 672

Brown R.D., Godfrey P.D., Storey J.W.V., Bassez M.-P., Robinson B.J., Batchelor R.A., McCulloch M.G., Rydbeck O.E.H., Hjalmarson A.G. 1979, *MNRAS*, 186, 5P

Brown R.D., Crofts J.G., Godfrey P.D., McNaughton D., Pierlot A.P. 1988, *J. Mol. Str.*, 190, 185

Combes F., Rieu N.Q., Wlodarczak G. 1996, *A&A*, 318, 618

Creswell R. A., Schwendeman R. H., 1977, *J. Mol. Spec.*, 64, 295

Dickens J.E., Irvine W.M., Ohishi M., Ikeda M., Ishikawa S., Nummelin A., Hjalmarson A. 1997, *ApJ*, 498, 753

Friedel D. N., Snyder L. E., Turner B. E., Remijan A., 2004, *ApJ*, 600, 234

Godfrey P. D., Brown R. L., Rodgers , 1996, *J. Mol. Str.*, 376, 65

Hollis J.M., Snyder L.E., Suenram R.D., Lovas F.J. 1980, *ApJ*, 241, 1001

Hollis J. M., Vogel S. N., Snyder L. E., Jewell P. R., Lovas F. J., 2001, *ApJ*, 554, L81

Hollis J. M., Pedelty J. A., Snyder L. E., Jewell P. R., Lovas F. J., Palmer P., Liu S.-Y., 2003a, *ApJ*, 588, 353

Hollis J.M., Pedelty J.A., Boboltz D.A., Liu S.-Y., Snyder L.E., Palmer P., Lovas F.J., Jewell P.R., 2003, *ApJ*, 596, L235

Hunt-Cunningham M.R., Jones P.A., 2004, in *Bioastronomy 2002: Life Among the Stars*, IAU Symposium 213, eds. R. Norris & F. Stootman, p 159

Joyce G. et al. 1984. *Nature* 310, 602

Kuan Y.-J., Mehringer D.M., Snyder L.E., 1996, *ApJ*, 459, 619

Kuan Y., Charnley S. B., Huang H., Tseng W., Kisiel Z., 2003, *ApJ*, 593, 848

Kuan Y., Charnley S. B., Huang H., Kisiel Z., Ehrenfreund P., Tseng W., Yan C., 2004, *AdSpR*, 33, 31

Kuan Y.-J., Huang H.-C., Charnley S.B., Tseng W.-L., Snyder L.E., Ehrenfreund P., Kisiel Z., Thorwirth S., Bohn R.K., Wilson T.L. 2004b, in *Bioastronomy 2002: Life Among the Stars*, IAU Symposium 213, eds. R. Norris & F. Stootman, p 185

Lovas F.J., Kawashima Y., Grabow J-U, Suenran R.D., Fraser G.T., Hirota E. 1995, *ApJ*, 455, L201

Liu S., Mehringer D. M., Snyder L. E., 2001, *ApJ*, 552, 654

Liu S., Snyder L. E., 1999, *ApJ*, 523, 683

Miao Y., Snyder L. E., 1997, *ApJ*, 480, L67

Miao Y., Snyder L.E, Kuan Y.-J., Lovas F.J. 1994, *Bull. Am. Astron. Soc.*, 26, 906

Müller H. S. P., Thorwirth S., Roth D. A., Winnewisser G., 2001, *A&A*, 370, L49

Nummelin A., Bergman P., Hjalmarson A., Friberg P., Irvine W. M., Millar T. J., Ohishi M., Saito S., 1998, *ApJS*, 117, 427

Pei C. C., Liu S., Snyder L. E., 2000, *ApJ*, 530, 800

Pickett H. M., Poynter R. L., Cohen E. A., Delitsky M. L., Pearson J. C., Müller H. S. P., 1998, *J. Quant. Spectrosc. & Rad. Transfer*, 60, 883

Rohlfs K., Wilson T. L., 2004, *Tools of radio astronomy*, 4th rev. Berlin: Springer

Snyder L. E., 1997, *OLEB*, 27, 115

Snyder L. E., et al., 2005, *ApJ*, 619, 914

Snyder L.E., Hollis J.M., Suenram R.D., Lovas F.J., Brown L.W., Buhl D. 1983, *ApJ*, 268, 123

Sorrell W.H. 2001, *ApJ*, 555, L129

Swalen D. R., Herschbach J. D., 1957, *J. Chem. Phys.*, 27, 100

Turner B.E. 1989, *ApJS*, 70, 539

Wirick, S., Flynn, G. J., Jacobsen, C., & Keller, L. P. 2006, 37th Annual Lunar and Planetary Science Conference, 37, 1418

This paper has been typeset from a *TeX/ L<sup>A</sup>TeX* file prepared by the author.